Virtual Element Method for Thermomechanical Problems in Electronic Packaging

Sishuai Li
Institute of Electronics Packaging Technology and Reliability
Beijing University of Technology
Beijing, China
lisishuai@emails.bjut.edu.cn

Yanpeng Gong*
Institute of Electronics Packaging Technology and Reliability
Beijing University of Technology
Beijing, China
yanpeng.gong@bjut.edu.cn

Fei Qin
Institute of Electronics Packaging Technology and Reliability
Beijing University of Technology
Beijing, China
qfei@bjut.edu.cn

Pei Chen
Institute of Electronics Packaging Technology and Reliability
Beijing University of Technology
Beijing, China
peichen@bjut.edu.cn

***Abstract*—Electronic packaging transforms semiconductor devices into functional products, with the Finite Element Method (FEM) serving as a reliable technique for structural reliability analysis. This paper introduces a virtual element method (VEM) for thermomechanical coupling problems in electronic packaging. VEM's mesh flexibility accepts arbitrary polygon shapes, simplifying complex geometry discretization. Our approach employs non-matching mesh generation—combining refined meshes for small-scale regions with coarser meshes for larger areas—reducing element count and computational demands. Additionally, VEM eliminates the need for explicit spatial basis functions, enhancing calculation accuracy and efficiency. Numerical examples verify the method's effectiveness, demonstrating that VEM provides an efficient, accurate approach for analyzing thermomechanical coupling in multi-scale electronic packaging structures.**

Keywords—Virtual Element Method, Non-matching mesh, Thermomechanical coupling

I. INTRODUCTION

Electronic packaging technology is evolving toward integration, miniaturization, and higher density, creating pronounced geometric multi-scale characteristics. As 3D integrated circuits become more compact with increased power density, electronic devices face multiple complex thermal and mechanical loads [1], which account for over 55% of device failures [2]. Analyzing thermal conduction and mechanical interaction is therefore essential for ensuring electronic packaging reliability.

Numerical analysis techniques, offering simple implementation and accurate calculation, are widely used for electronic packaging reliability problems. Various numerical simulation methods have been developed to study these reliability issues in practice. Feng and colleagues developed the stable node-based smoothed finite element algorithm (SNS-FEM), verifying its validity for coupled electrical-thermal-force analysis of IGBT modules [3]. Oukaira et al. used COMSOL for transient thermal analysis of system-in-package technology to study underlying layer effects on thermal models [4]. Gong et al. [5][6] introduce a thermo-mechanical coupled phase-field model for analyzing mechanical performance and damage evolution in electronic packaging interconnect structures. In [7], Gong et al. introduce a coupled finite element – boundary element (FEM – BEM) method for transient elastic dynamic analysis, offering a computationally efficient alternative for studying electronic packaging structures with complex geometries. Vallepuga-Espinosa et al. [8] developed a boundary element formulation for thermoelastic contact problems in 3D microelectronic packages, demonstrating its effectiveness in predicting thermomechanical behavior at high temperatures and low clamping pressures. Despite these advancements, existing methods still face significant challenges in accurately analyzing geometrically multi-scale electronic package structures. For finite element simulations, multi-scale structures (combining large and small dimensions in the same model) require extremely fine meshes and elements of varying sizes for transitions. This dramatically increases mesh quantities in electronic packaging simulation models with micro-to-centimeter scale spans, potentially involving millions of elements, thereby increasing computational burden and affecting result convergence. Moreover, some methods are only applicable to specific structures or problems.

In 2013, Veiga et al. [9] proposed the Virtual Element Method (VEM), an innovative extension of the Finite Element Method that accommodates arbitrarily shaped polygonal elements. VEM's mesh flexibility enables non-matching mesh construction, simplifying complex geometry meshing and offering significant advantages for fracture mechanics [10] and contact mechanics [11] problems. This paper applies the Virtual Element Method (VEM) to thermomechanical coupling in geometrical multi-scale electronic packaging structures using non-matching mesh discretization. Fine meshes address complex small-scale regions while coarser meshes handle larger-scale regions, integrating these parts into a single model. This approach ensures high-accuracy local simulation while reducing element count and computational cost—a significant advantage for electronic package structural analysis.

II. VEM THEORY FOR THERMOMECHANICAL COUPLING

For thermoelastic problems using VEM, we first determine the structure's steady-state temperature field, then apply it as a thermal load to analyze thermal stresses. The process involves solving the heat transfer problem to obtain temperature distribution, followed by solving the

mechanical problem. We begin with the theoretical VEM framework for heat conduction analysis.

A. VEM formulation for heat conduction

The weak form of the temperature field equilibrium equation is

$$a_T(T,\varphi)=\ell_T(\varphi),\varphi\in\gamma_T \tag{1}$$

where γ_T is the temperature solution space.

The bilinear and linear forms are defined as

$$a_T(T,\varphi)=\int_\Omega \nabla T\cdot\nabla\varphi d\Omega \tag{2}$$

$$\ell_T(\varphi)=\int_{\partial\Omega}\varphi\cdot\bar{q}d\Omega \tag{3}$$

For the heat conduction problem, the virtual element function space is

$$V_T(E)=\left\{T\in H^1(E):T|_{\partial E}\in P_k(E),T=\overline{T}\ on\ \partial\Omega_T\right\} \tag{4}$$

where $P_k(E)$ denotes the space of polynomial functions of degree not exceeding *k*, with $k=1$ in this work.

In the polynomial space, the scaling factor ξ and η are defined as

$$\xi=\left(\frac{x_1-\bar{x}_1}{h_E}\right),\qquad \eta=\left(\frac{x_2-\bar{x}_2}{h_E}\right). \tag{5}$$

where x_1 and x_2 represent position coordinates in the two-dimensional space, $\bar{x}=(\bar{x}_1,\bar{x}_2)$ denotes the centroid of element E, and h_E represents the maximum distance between any two nodes in element E.

The basis functions of the polynomial space $P_k(E)$ are defined as

$$P_k(E)=\{1,\ \xi,\ \eta\} \tag{6}$$

For each element with n_v vertices, define a local space $\vartheta_T(T)\in V_T(E)$, the number of degrees of freedom of the element is $n_d=n_v$. The basis functions of a local VEM space along one dimension are denoted as $\{\psi_i\}_{i=1,2,3\cdots,\ n_d}$.

The projection operator, a key component defined as $\Pi:\vartheta_T(T)\to P_k(E)$ is constructed separately within each element and satisfies the following orthogonality conditions

$$a_E(\varphi^h-\Pi\varphi^h,p)=0\quad \varphi^h\in\vartheta_T(E),\ \forall p\in P_K(E) \tag{7}$$

For $T^h,\varphi^h\in\vartheta_T(E)$, the discrete bilinear form of each element E is:

$$\begin{aligned}&a_E(T^h,\varphi^h)=a_E(T^h-\Pi T^h+\Pi T^h,\varphi^h-\Pi\varphi^h+\Pi\varphi^h)\\&=a_E(\Pi T^h,\Pi\varphi^h)+a_E(T^h-\Pi T^h,\varphi^h-\Pi\varphi^h)\end{aligned} \tag{8}$$

where the right-hand side's first term is the consistency term and the second term is the stability term.

The element temperature stiffness matrix is

$$\mathrm{K}_E^T=\mathrm{K}_E^{Tc}+\mathrm{K}_E^{Ts} \tag{9}$$

where K_E^{Tc} is the coordination stiffness matrix related to the projection operator coordination. K_E^{Ts} is the stability stiffness matrix.

Because $\Pi\psi_i\in P_k(E)$, we define $\Pi\psi_i$ as a linear combination of p_α

$$\Pi\psi_i=\sum_{\beta=1}^{n_k}s_{i,\beta}p_\alpha\qquad p_\alpha\in\mathrm{P}_k(E) \tag{10}$$

where $s_{i,\beta}$ is a constant parameter. Defining projection operator $\tilde{\mathbf{\Pi}}$ as the matrix of $s_{i,\beta}$, the matrix form of Eq. (10) becomes

$$\Pi\psi=p_\alpha\tilde{\mathbf{\Pi}} \tag{11}$$

Based on Eq. (2), Eq. (7) can be derived as

$$\int_E\nabla\varphi^h\cdot\nabla p\ dE=\int_E\nabla\Pi\varphi^h\cdot\nabla p\ dE,\quad\forall p\in\mathrm{P}_K(E) \tag{12}$$

Using Green's formula, Eq. (11) can be expressed as

$$\int_E\nabla\Pi\varphi^h\cdot\nabla p\ dE=\int_{\partial E}\varphi^h\cdot\frac{\partial p}{\partial n}d\partial E-\int_E\varphi^h\cdot\nabla(\nabla p)dE \tag{13}$$

According to Eqs. (11), (12) and (13), we obtain

$$\int_E\nabla p_\alpha\cdot\nabla p_\alpha dE\tilde{\mathbf{\Pi}}=\int_{\partial E}\nabla p_\alpha\cdot n\cdot\psi\ d\partial E-\int_E\psi\cdot\nabla(\nabla p_\alpha)\ dE \tag{14}$$

We define

$$G=\int_E\nabla p_\alpha\cdot\nabla p_\alpha dE \tag{15}$$

$$B=\int_{\partial E}\nabla p_\alpha\cdot n\cdot\psi\ d\partial E-\int_E\psi\cdot\nabla(\nabla p_\alpha)\,dE \tag{16}$$

The matrix representation of the projection operator $\tilde{\mathbf{\Pi}}$ is

$$\tilde{\mathbf{\Pi}}=\mathbf{G}^{-1}\mathbf{B} \tag{17}$$

Define matrix $\mathbf{D}\in\mathbb{R}^{n_d\times n_\alpha}$ as the values of polynomial basis p_α at degrees of freedom locations:

$$D_{i\alpha}=\mathrm{dof}_i(p_\alpha),\ \ i=1,2,3,\cdots,n_d\ ,\ \alpha=1,2,3 \tag{18}$$

The matrix $\mathbf{G}$ can be expressed as

$$\mathbf{G}=\mathbf{BD} \tag{19}$$

The coordination stiffness matrix can be expressed as

$$K_E^{Tc}=a\left(\Pi\psi,\Pi\psi\right)=\int_E\nabla\Pi\psi\cdot\nabla\Pi\psi dE=\tilde{\mathbf{\Pi}}^T\mathbf{G}\tilde{\mathbf{\Pi}} \tag{20}$$

The stabilization stiffness matrix expression is

$$\mathrm{K}_E^s=\tau^h tr\left(k_E^c\right)(\mathbf{I}-\mathbf{\Pi})^\intercal(\mathbf{I}-\mathbf{\Pi}) \tag{21}$$

where τ^h is a user-defined parameter, tr(·) is the tracking operator, and I represents the identity matrix. $\mathbf{\Pi}$ is the matrix of the projection operator $\vartheta_T(T)$ acting on itself, expressed as

$$\mathbf{\Pi} = D\tilde{\mathbf{\Pi}}. \tag{22}$$

Assembling all element stiffness matrices into a global stiffness matrix

$$K^T = \sum_E K_E^T \tag{23}$$

Finally, solving the system of linear equations $K^T T = q$ with boundary conditions yields the temperature field.

B. VEM formulation for thermoelastic

The weak form of the force field equilibrium equation is

$$a_T(u,\upsilon) = \ell(\upsilon), \upsilon \in \gamma_u \tag{24}$$

where γ_u denotes the displacement field space.

The bilinear and linear forms are defined as

$$a(u,\upsilon) = \int_\Omega \sigma(u) : \varepsilon(\upsilon) d\Omega \tag{25}$$

$$\ell(\upsilon) = \int_\Omega \upsilon \cdot f \, d\Omega + \int_{\partial\Omega} \upsilon \cdot \bar{t} d\partial\Omega \tag{26}$$

For the linear elasticity problem, the vector function space of VEM is

$$\begin{aligned} \mathrm{V}_u(E) \coloneqq \Big\{ & \upsilon^h \in [H^1(E)]^2 : \upsilon^h\big|_{\partial E} \in [C^0(\partial \mathrm{E})]^2, \\ & \upsilon^h\big|_E \in \mathrm{M}_k(\mathrm{E}), \Delta\upsilon^h\big|_E \in \mathrm{M}_{k-2}(E) \Big\} \end{aligned} \tag{27}$$

where $\mathrm{M}_k(E) = \begin{pmatrix}1\\0\end{pmatrix}, \begin{pmatrix}0\\1\end{pmatrix}, \begin{pmatrix}-\wp\\ \zeta\end{pmatrix}, \begin{pmatrix}\wp\\ \zeta\end{pmatrix}, \begin{pmatrix}\zeta\\0\end{pmatrix}, \begin{pmatrix}0\\ \wp\end{pmatrix}$ is the space of polynomial functions with degree not exceeding *k*.

For an element with n_v vertices, the local virtual element space is $V^h(E) \in \mathrm{V}_u(E)$. For two-dimensional vector problems, the polygonal element has $n_d = 2n_v$ degrees of freedom. The basis functions of a local virtual element space along one dimension are denoted $\{\varphi_i\}_{i=1,2,3\cdots,\ n_d}$. The basis functions ϕ are expressed as

$$\phi_1 = [\varphi_1, 0]^T, \phi_2 = [\varphi_2, 0]^T, \cdots, \phi_{2\,n_d} = [\varphi_{2\,n_d}, 0]^T \tag{28}$$

Define the projection operator $\Pi^\nabla : V_K(E) \to \mathrm{M}_k(E)$ satisfying the orthogonality condition

$$a_E(u^h - \Pi u^h, m) = 0, \qquad \forall m \in \mathrm{M}_k(E) \tag{29}$$

For $u^h, \upsilon^h \in V^h$, the bilinear form on the element is given by

$$\begin{aligned} & a_E(u^h, \upsilon^h) = a_E(u^h - \Pi u^h + \Pi u^h, \upsilon^h - \Pi\upsilon^h + \Pi\upsilon^h) \\ & = a_E(\Pi u^h, \Pi\upsilon^h) + a_E(u^h - \Pi u^h, \upsilon^h - \Pi\upsilon^h) \end{aligned} \tag{30}$$

We define $\Pi\phi_i$ as a linear combination of m_α

$$\Pi(\phi_i) = \sum_{\alpha=1}^{n_k} \omega_{i,\alpha} m_\alpha \qquad m_\alpha \in \mathrm{M}_k(E) \tag{31}$$

Based on the orthogonality condition, Eq. (31) can be derived as

$$a_E(\phi_i, m_\beta) = \sum_{\beta=1}^{n_k} \omega_{i,\beta} a_E(m_\alpha, m_\beta), \quad \forall m_\alpha \in \mathrm{M}_k(E) \tag{32}$$

The matrix representation of the projection operator is

$$\tilde{\mathbf{\Pi}}^\nabla = \bar{\mathbf{G}}^{-1}\bar{\mathbf{B}} \tag{33}$$

Using Green's formula, matrix $\bar{\mathbf{B}}$ can be expressed as

$$\bar{\mathbf{B}} = a_E(\phi_i, m_\beta) = \sum_{j=1}^{n_v} \frac{|e_j|}{2} \sum_{r=1}^{k+1} \varphi_i \cdot \left(\sigma(m_\alpha) | \cdot \hat{n}_{e_j}\right) \tag{34}$$

Define matrix $\bar{\mathbf{D}} \in \mathbb{R}^{2n_d \times n_k}$ as polynomial basis m_α values at degrees of freedom locations:

$$\bar{D}_{i\alpha} = \mathrm{dof}_i(m_\alpha), \ \ i = 1,2,3,\cdots,2n_d \ , \ \alpha = 1,2,3,\cdots,n_k \tag{35}$$

Matrix $\bar{\mathbf{G}}$ can be expressed as

$$\bar{\mathbf{G}} = \bar{\mathbf{B}}\bar{\mathbf{D}} \tag{36}$$

The element displacement stiffness matrix is

$$\mathrm{K}_E^u = \mathrm{K}_E^{uc} + \mathrm{K}_E^{us} \tag{37}$$

where $\mathrm{K}_E^{uc} = (\tilde{\mathbf{\Pi}}^\nabla)^T \bar{\mathbf{G}} \tilde{\mathbf{\Pi}}^\nabla$ is the coordination stiffness matrix, and $\mathrm{K}_E^s = \tau^h tr\left(k_E^c\right)(\mathbf{I} - \mathbf{\Pi}^\nabla)^{\mathrm{T}}(\mathbf{I} - \mathbf{\Pi}^\nabla)$ is the stabilization stiffness matrix.

The global displacement stiffness matrix is assembled from element displacement stiffness matrices as:

$$K^u = \sum_E K_E^u \tag{38}$$

We utilize the computed temperature field as a thermal load, then solve the system equation $K^u u = F$ to obtain the displacement field.

The VEM thermomechanical coupling analysis employs two sequential Matlab programs: first, the VEM heat conduction program calculates the model's temperature field; then, this temperature field serves as a thermal load for the VEM thermoelastic program to analyze thermal stress and displacement. Fig. 1 illustrates the complete VEM thermomechanical coupling analysis process.

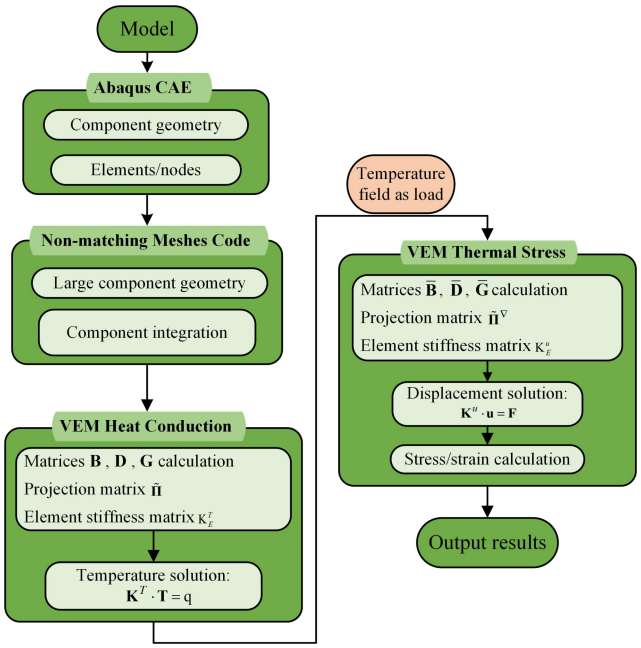

Fig. 1. VEM thermomechanical coupling analysis workflow

III. Mesh Strategy

The VEM offers exceptional mesh flexibility, simplifying transitions between multi-scale structural components. This makes it ideal for geometric multi-scale electronic packaging analysis. The non-matching meshing strategy isolates local mesh changes from the global structure, enhancing flexibility while significantly reducing mesh quantity.

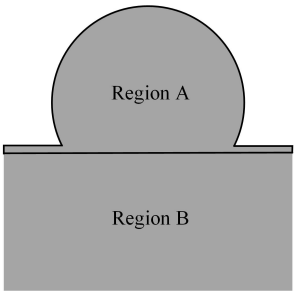

Fig. 2. Sphere structure with domain decomposition strategy

For the sphere structure in Fig. 2, engineering experience shows stress concentration typically occurs at sphere-plate junctions. To accurately capture this mechanical behavior, fine mesh is applied to these concentration regions. As shown in Fig. 3, a non-matching mesh strategy was implemented where structural components were independently meshed and interface nodes were directly transformed into polygonal elements. Complex geometrical components were initially built and meshed in Abaqus, with nodal information extracted from input files and imported into a custom Matlab program for non-conforming mesh generation and further processing.

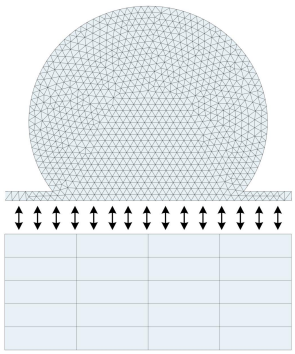

(a) Structural mesh distribution

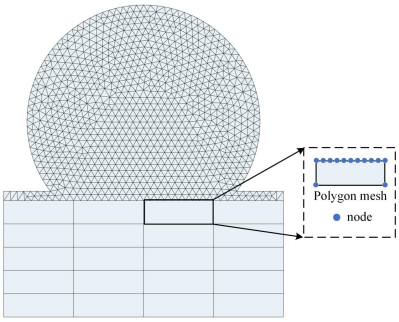

(b) Interface polygonal element

Fig. 3. Sphere structure with non-matching mesh

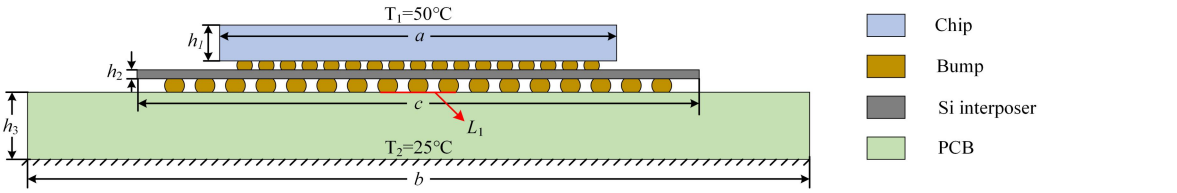

Fig. 4. 2.5D packaging geometric model and boundary conditions

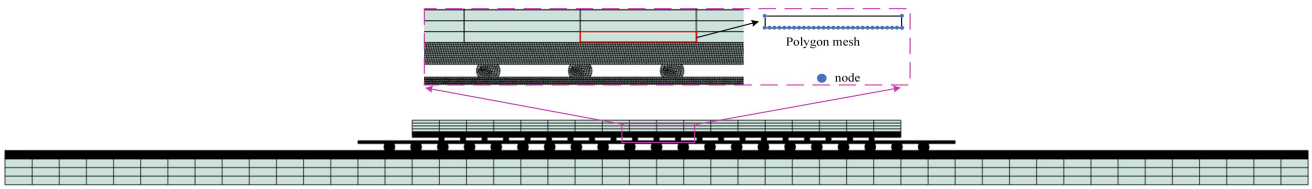

Fig. 5. Multi-scale packaging structure with non-matching mesh

IV. Numerical Example

In this paper, the thermomechanical coupling problem of a 2.5D silicon-interposer packaging structure verifies the proposed method's reliability. Fig. 4 illustrates the model geometry and boundary conditions. The geometric parameters are: $a = 18$ mm , $b = 48$ mm , $c = 22$ mm , $h_1 = 0.6$ mm , $h_2 = 0.1$ mm , $h_3 = 1.2$ mm . The solder joints on the Si-interposer's upper side are $R_1 = 0.1$ mm , $H = 0.12$ mm , and on the lower side are $R_1 = 0.2$ mm , $H = 0.24$ mm . TABLE I summarizes simulation material properties. Fixed constraints ($u_x = u_y = 0$) at the model's bottom surface, with temperature of 50 °C on the upper surface and 25 °C on the lower surface. Other boundaries are thermally insulated ($\Delta T \cdot n = 0$).

TABLE I. Properties of Materials In 2.5D Packaging

Material	Material Parameters			
	***Young's modulus E* (MPa)**	***Poisson's ratio v***	***Thermal expansion α* ($^{\circ}C^{-1}$)**	***Thermal conductivity k* (W/m·K)**
Chip	131000	0.28	2.8×10^{-6}	150
Bump	25500	0.35	25×10^{-6}	67
Si	131000	0.28	2.8×10^{-6}	150
PCB	22000	0.15	18×10^{-6}	16.4

Fig. 5 illustrates non-matching mesh discretization for the packaging model. With significant geometric variations between the Bump and other components, non-matching mesh strategy increases element density near critical interfaces while reducing mesh density in less critical regions, improving computational efficiency.

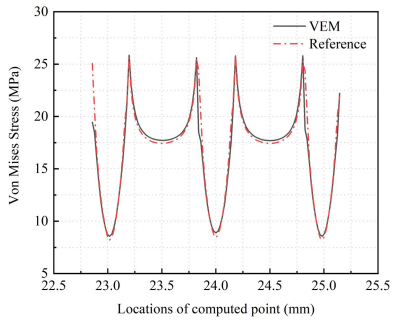

(a) Thermal stress distribution

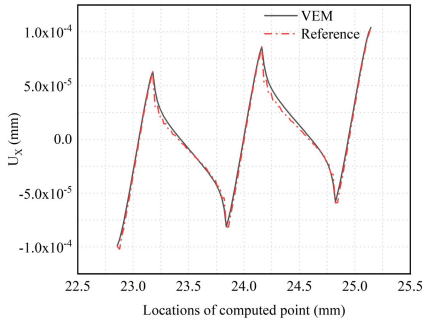

(b) Horizontal displacement (U_X) distribution

Fig. 6. VEM and Abaqus results comparison along line L_1

Fig. 6 compares stress and displacement distributions along line L_1 (highlighted in Fig. 4) between the proposed VEM and commercial finite element software Abaqus (using extremely fine mesh as a reliable reference). The close correspondence confirms that the proposed VEM successfully captures the electronic packaging structure's thermomechanical behavior.

Finally, we compared the computational time of the VEM algorithm across three different degrees of freedom configurations against finite element methods using equivalent element counts. The calculation time statistics are presented in TABLE II. As shown in the results, computation time increases with higher degrees of freedom for both methods. The VEM method requires less processing time than the FEM Matlab implementation.

TABLE II. Comparisons of Computation Time

Methods	Calculation Time		
	nDof=24426	**nDof=42906**	**nDof=60650**
VEM	10.6	19.23	34.34
FEM (Matlab)	16.99	36.6	56.46

V. Conclusions

This paper proposes a Virtual Element Method (VEM) for solving thermomechanical coupling problems. Our non-matching mesh strategy avoids transition meshing and substantially reduces element count while maintaining computational accuracy, proving particularly effective for multi-scale electronic packaging structures. The numerical example demonstrates that VEM accurately solves thermomechanical coupling problems in electronic packaging.

Acknowledgment

This research is supported by the National Natural Science Foundation of China (No. 12002009), R&D Program of Beijing Municipal Education Commission (No. KM202110005032).

References

[1] Y. Gong, F. Qin, C. Dong, J. Trevelyan, An isogeometric boundary element method for heat transfer problems of multiscale structures in electronic packaging with arbitrary heat sources, Applied Mathematical Modelling 109 (2022) 161–185.

[2] Z. He, Y. Yan, Z. Zhang, Thermal management and temperature uniformity enhancement of elec-tronic devices by micro heat sinks: A review, Energy 216 (2021) 119223.

[3] S. Feng, Y. Guo, G. Królczyk, X. Han, A. Incecik, Z. Li, An engineered solution to multi-physics of insulated gate bipolar transistor module considering electrical-thermal-mechanical coupling effect, Advances in Engineering Software 175 (2023) 103365.

[4] Oukaira A, Said D, Zbitou J, et al. Transient thermal analysis of system-in-package technology by the finite element method (FEM)[C]//2022 International Conference on Microelectronics (ICM). IEEE, 2022: 30-33.

[5] Gong Y, Kou Y, Yue Q, Zhuang X, Valizadeh N, Qin F. Rabczuk T. A phase-field study on thermo-mechanical coupled damage evolution and failure mechanisms of sintered silver interconnections. Engineering Fracture Mechanics 2025, 320: 111039.

[6] Gong Y, Kou Y, Yue Q, Zhuang X, Qin F, Wang Q, Rabczuk T. The application of thermomechanically coupled phase-field models in electronic packaging interconnect structures. International Communications in Heat and Mass Transfer 2024, 159: 108033.

[7] Gong Y, He Y, Hu H, Zhuang X, Qin F, Xu H, Rabczuk T. A coupled finite element–boundary element method for transient elastic dynamic analysis of electronic packaging structures. Engineering Structures 2025, 326: 119500.

[8] Vallepuga-Espinosa J, Ubero-Martínez I, Rodríguez-Tembleque L, et al. A boundary element procedure to analyze the thermomechanical contact problem in 3D microelectronic packaging. Engineering Analysis with Boundary Elements, 2020, 115: 28-39.

[9] L. Beirão da Veiga, F. Brezzi, A. Cangiani, G. Manzini, L. D. Marini, A. Russo, Basic principles of virtual element methods, Mathematical Models and Methods in Applied Sciences 23 (01) (2013)199–214.

[10] A. Hussein, F. Aldakheel, B. Hudobivnik, P. Wriggers, P.-A. Guidault, O. Allix, A computational framework for brittle crack-propagation based on efficient virtual element method, Finite elements in analysis and design 159 (2019) 15–32.

[11] M. Cihan, B. Hudobivnik, J. Korelc, P. Wriggers, A virtual element method for 3D contact problems with non-conforming meshes, Computer Methods in Applied Mechanics and Engineering 402 (2022) 115385.